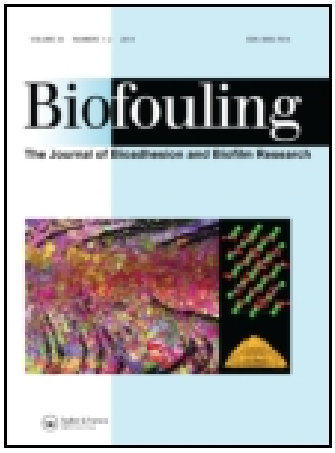

Biofouling: The Journal of Bioadhesion and Biofilm Research
Publication details, including instructions for authors and subscription information:
http://www.tandfonline.com/loi/gbif20

Discrimination between random and non-random processes in early bacterial colonization on biomaterial surfaces: application of point pattern analysis

Daniel Siegismund[ab], Anja Schroeter[b], Claudia Lüdecke[cd], Andreas Undisz[a], Klaus D. Jandt[c], Martin Roth[d], Markus Rettenmayr[a], Stefan Schuster[b] & Sebastian Germerodt[b]

[a] Otto Schott Institute of Materials Research (OSIM), Friedrich Schiller University Jena, Jena, Germany

[b] Department of Bioinformatics, Friedrich Schiller University Jena, Jena, Germany

[c] Otto Schott Institute of Materials Research (OSIM), Friedrich Schiller University Jena, Jena, Germany

[d] Leibniz Institute for Natural Product Research and Infection Biology, Hans Knöll Institute (HKI), Bio Pilot Plant, Jena, Germany

Published online: 20 Oct 2014.

To cite this article: Daniel Siegismund, Anja Schroeter, Claudia Lüdecke, Andreas Undisz, Klaus D. Jandt, Martin Roth, Markus Rettenmayr, Stefan Schuster & Sebastian Germerodt (2014) Discrimination between random and non-random processes in early bacterial colonization on biomaterial surfaces: application of point pattern analysis, Biofouling: The Journal of Bioadhesion and Biofilm Research, 30:9, 1023-1033, DOI: 10.1080/08927014.2014.958999

To link to this article: http://dx.doi.org/10.1080/08927014.2014.958999

Biofouling, 2014
Vol. 30, No. 9, 1023–1033, http://dx.doi.org/10.1080/08927014.2014.958999

Taylor & Francis
Taylor & Francis Group

Discrimination between random and non-random processes in early bacterial colonization on biomaterial surfaces: application of point pattern analysis

Daniel Siegismund[a,b], Anja Schroeter[b], Claudia Lüdecke[c,d], Andreas Undisz[a], Klaus D. Jandt[c], Martin Roth[d], Markus Rettenmayr[a], Stefan Schuster[b] and Sebastian Germerodt[b]*

[a]*Otto Schott Institute of Materials Research (OSIM), Friedrich Schiller University Jena, Jena, Germany;* [b]*Department of Bioinformatics, Friedrich Schiller University Jena, Jena, Germany;* [c]*Otto Schott Institute of Materials Research (OSIM), Friedrich Schiller University Jena, Jena, Germany;* [d]*Leibniz Institute for Natural Product Research and Infection Biology, Hans Knöll Institute (HKI), Bio Pilot Plant, Jena, Germany*

(*Received 6 May 2014; accepted 20 August 2014*)

The dynamics of adhesion and growth of bacterial cells on biomaterial surfaces play an important role in the formation of biofilms. The surface properties of biomaterials have a major impact on cell adhesion processes, eg the random/non-cooperative adhesion of bacteria. In the present study, the spatial arrangement of *Escherichia coli* on different biomaterials is investigated in a time series during the first hours after exposure. The micrographs are analyzed *via* an image processing routine and the resulting point patterns are evaluated using second order statistics. Two main adhesion mechanisms can be identified: random adhesion and non-random processes. Comparison with an appropriate null-model quantifies the transition between the two processes with statistical significance. The fastest transition to non-random processes was found to occur after adhesion on PTFE for 2–3 h. Additionally, determination of cell and cluster parameters *via* image processing gives insight into surface influenced differences in bacterial micro-colony formation.

Keywords: bacterial colonization; point-pattern analysis; bacterial adhesion; biofilm; biomaterials; image processing

Introduction

The formation of biofilms on abiotic surfaces is a persistent and complex phenomenon. In the fields of engineering, natural science and medicine it is very important to understand and control this phenomenon. In particular, implant materials that are intended to substitute human hard and soft tissue are often prone to biofilm formation on their surface (Gristina 1987; Costerton et al. 1999). Biofilms are known to initiate an infection at the site of the implant, the so-called 'biomaterial-associated infection', frequently necessitating total implant replacement (Gottenbos et al. 2002). Adhesion of bacteria to the biomaterial surface and growth in a monolayer are the first crucial stages in biofilm formation (Katsikogianni & Missirlis 2004). Intervention in the processes at these early stages, eg *via* the application of suitable surface modifications, has been found to be effective (Renner & Weibel 2011). Extensive studies have been carried out to investigate the influence of surface chemistry (Katsikogianni & Missirlis 2004; Ponche et al. 2010) or surface topography (Medilanski et al. 2002; Giraldez et al. 2010; Ivanova et al. 2010; Singh et al. 2011; Siegismund et al. 2014) on the first stages of biofilm formation, particularly bacterial attachment to the surface. In contrast, relatively few studies focus on the influence of the surface on subsequent bacterial monolayer formation (Barton et al. 1996; Gottenbos et al. 2000; Ploux et al. 2007) or the transition of adhesion mechanisms eg from random to cooperative adhesion (Van der Mei et al. 1993; Beloin et al. 2008). The proliferation of bacterial cells on the surface may be microbiological evidence for a switch from the planktonic to the biofilm lifestyle, and implies a substantial change in the inherent metabolic processes of the cells (Busscher et al. 2012). The initial monolayer growth accompanied by the production of extracellular polymeric substances (EPS) is also a factor in the pathogenesis of a bacterial biofilm. This monolayer is the 'binding' layer between the biofilm and the abiotic surface (Gottenbos et al. 2000). Real-time cell tracking studies have been carried out to investigate hypotheses on the attachment of *Pseudomonas aeruginosa* to surfaces (Gibiansky et al. 2010; Zhao et al. 2013).

In reality, the processes of random adhesion, cooperative adhesion and growth occur concurrently both *in vitro* and *in vivo*. Thus, it is difficult to separate these processes quantitatively. Qualitative analysis of bacterial growth kinetics using subjective measures, eg by identifying different slopes of surface coverage evolution curves, could assist in distinguishing different surface induced processes, but this is not a quantitative measure

*Corresponding author. Email: sebastian.germerodt@uni-jena.de

or statistically verified (Ploux et al. 2007). A crucial factor is the time at which the dominant form of bacterial colonization of the surface changes from random attachment to non-random processes. Non-random processes generally lead to an increased local density of bacteria, facilitating local biofilm formation. Quantitative assessment of the time that is required for the transition from random to non-random processes (cooperative adhesion or division) on biomaterials would provide a valuable new measure for determining the performance of a biomaterial. Thus, a suitable biomaterial surface should not only have resistance to bacterial attachment, but also should be assessed for its behavior in monolayer growth and micro-colony formation.

One possible method of achieving such quantification is the use of a second-order statistical method, in particular the pair-correlation function (PCF) or O-ring statistics. This is designed for analyzing the spatial distribution of points within a region of interest and is capable of detecting any significant occurrence of clustered points (Wiegand & Moloney 2004). Originally developed for statistical mechanics (McQuarrie 1975), it is frequently used in ecology to describe spatial patterns (Wiegand & Moloney 2004; Law et al. 2009; Schleicher et al. 2011). In biofilm research, the PCF was introduced in the early 1990s and is occasionally used to study co-adhesion of different bacterial species to biomaterial surfaces (Sjollema & Busscher 1990; Sjollema et al. 1990; Bos et al. 1994; Schillinger et al. 2012).

In the present study the spatial distribution of *Escherichia coli* on four different biomaterial surfaces (titanium dioxide (TiO_2), tissue culture polystyrene (TCPS), polytetrafluoroethylene (PTFE), and glass) was analyzed in a time series during the first few hours after exposing the biomaterial surfaces to the bacterial suspension. Comparison of the evaluated PCF for all acquired points in time with random distributions of the respective point density (null-model) unravels the dependency of the colonization process of *E. coli* on the substratum material. In agreement with a previous work on stainless steel (Hamilton et al. 1995), this study confirms that the initial attachment process of *E. coli* is fully random, even on fundamentally different biomaterials.

The result of the PCF analysis is a quantitative and statistically significant separation of random and non-random surface induced phenomena in the early stages of biofilm formation that has, to the authors' knowledge, not been achieved in previous work.

Materials and methods

Experimental methods

Bacterial adhesion kinetics were investigated on TiO_2, TCPS, PTFE and silicate glass surfaces. The points in time chosen for measurements were 1–48 h after exposure of the biomaterial surfaces to the bacterial suspension. *E. coli* EC081 was cultured in a continuous culture (chemostat) that was used for inoculation of a biofilm reactor (non-constant depth film fermenter; nCDFF) to study bacterial adhesion.

Details of the applied experimental protocol can be found in the Supplementary information [Supplementary information is available *via* a multimedia link on the online article webpage] and in Lüdecke et al. (2013, 2014).

Microscopy

A confocal laser scanning microscope (CLSM, Zeiss LSM 510 Meta, Carl Zeiss MicroImaging, Jena, Germany), equipped with an Argon laser (488 nm) and a 63 × NA 1.3 oil immersion lens objective (Zeiss PLANAPOCHROMAT®) was used for imaging the bacterial cells. Applying a 1.5-fold digital zoom resulted in a basic field of view for each image of 71.4 µm × 71.4 µm. CLSM imaging was carried out at five different randomly chosen locations on each sample using three biological replicates, giving a total of 15 different locations of analysis per point in time per material. Since the required quantity for a fully reliable statistical analysis is not obtained directly, for all analytical/mathematical operations that were performed on the measured quantities, a propagation of uncertainty was applied according to Taylor (1997).

Image processing

For applying point pattern analysis to the CLSM images, it is necessary to represent the bacterial cells as single points. Thus, specific image pre-processing is necessary, particularly to distinguish between non-spherical bacterial cells as *E. coli* within clusters. All image processing procedures are implemented in the numerical computing environment MATLAB (The MathWorks, Inc., Natick, MA, USA). In the present study, the point approximation is incorporated using the center of mass of the bacterium as a representation, which is a sufficiently accurate method under the present conditions (Wiegand et al. 2006). In Figure 1 an example of the image processing routine is shown.

The first step in the image processing routine is to separate the image into background and bacteria to achieve a binary image. In this study, an automatic thresholding algorithm based on Otsu's (1979) method was used (see Figure 1b). All bacteria adjoining the image border are not considered in the following processing steps.

It is a complex challenge to specify the centers of mass of single bacterial cells within bacterial clusters.

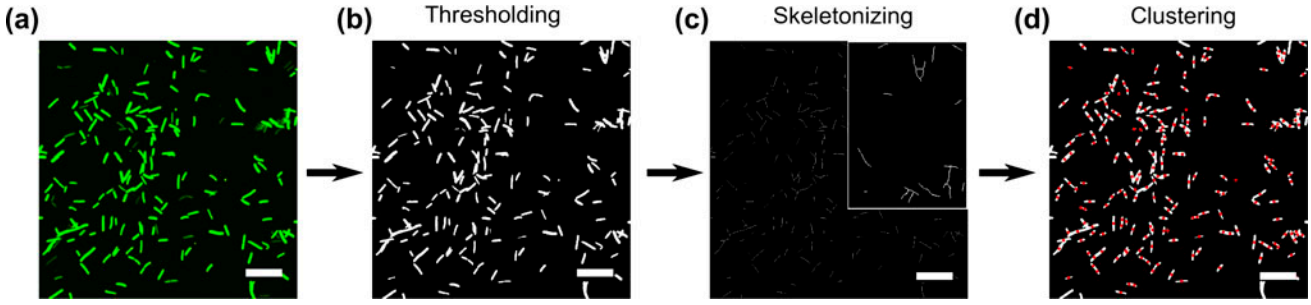

Figure 1. Image processing routine for the determination of the center of mass for each bacterium (TiO_2 -9 h). (a) Raw CLSM image; (b) binary image after Otsu thresholding; (c) topologically skeletonized image for cluster size determination; (d) final result: centers of mass for each bacterium (red). Scale bar = 10 µm.

A topological skeletonizing algorithm for bacterial clusters is incorporated to determine the branching points and subsequently the number of bacteria within the clusters (which is the number of branching points plus one) (Grivet et al. 1999). The centers of mass are then determined by a Gustafson–Kessel clustering algorithm with the determined class size (= number of bacteria) (Gustafson & Kessel 1979).

In order to evaluate the detection accuracy of the number of bacteria within the clusters, three different images at four different points in time per substratum material were compared, with manual counting as the gold standard (see Figure S1).

Laser background scattering occurring during CLSM imaging is different on the investigated materials. Nevertheless the image processing routine is capable of addressing this issue without leading to incorrect calculations (see Figure S2). Furthermore, the performance comparison of the automatic image processing with manual counting shows a mean relative deviation of only 3.8% (see Figure S1).

Point pattern analysis

All steps in the point pattern analysis were performed using the programming language R with the Spatstat package (Baddeley & Turner 2005).

PCF characterizes particle density at a particular distance to a reference particle. All identified centers of mass for a single bacterium were passed sequentially, and rings (annuli) with a thickness *dr* in an increasing distance *r* were generated. A schematic illustration is given in Figure 2.

The PCF is determined mathematically as a ratio of two densities (Sjollema & Busscher 1990):

$$g(r) = \frac{\rho(r, dr)}{\rho_0} \tag{1}$$

with:

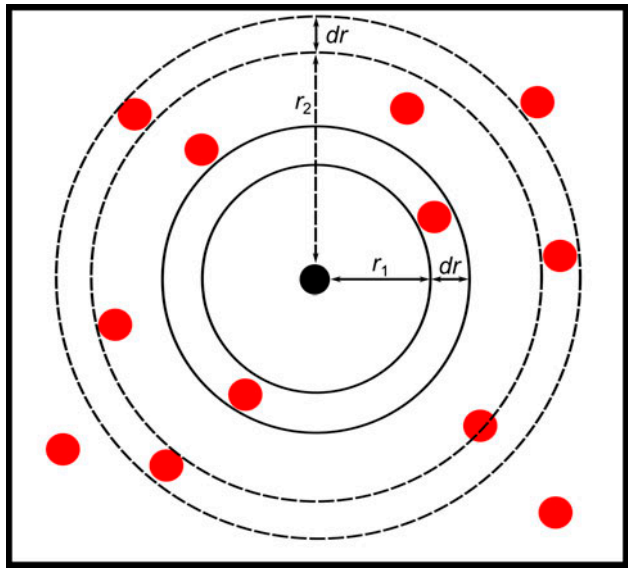

Figure 2. Schematic illustration of the principle of PCF determination for two different rings (annuli); r_1 and r_2 are examples of the changing radius; *dr* is the constant ring thickness; red dots represent the centers of mass of the bacterial cells; the black dot marks the selected reference center.

$$\rho(r, dr) = \frac{N(r, dr)}{A(r, dr)} \tag{2}$$

$$\rho_0 = \frac{N_W}{A_W}, \tag{3}$$

where N(*r*,*dr*) is the number of the bacterial centers (bacterial cells) residing within the respective ring of area A(*r*,*dr*) and N_w is the number of all bacterial centers within the whole image area A_w.

Generally, *g*(*r*) describes the local bacterial density, in a given radius *r* (see Figure 2), relative to the bacterial density within the overall image. Thus, if the density $\rho(r, dr)$ within one ring is similar to the density in the entire image (ρ_0), the relation *g*(*r*) = 1 holds and the relative density equals the bacterial density in the whole image.

For $g(r) > 1$, the local bacterial density within the respective ring is higher than that estimated from the overall density. By analogy, for $g(r) < 1$ the distance r is less likely. Edge effects are treated using an isotropic edge correction (Ripley 1977; Wiegand & Moloney 2004).

The PCFs of random and non-random processes are inherently different (Bos et al. 1994). The expected value of the $g(r)$ of a random process is 1, implying that the density of bacteria in the respective ring is similar to that averaged over the whole image (see Equation 1) (Sjollema & Busscher 1990). For non-random processes, the values of $g(r)$ differ significantly from 1 (Schillinger et al. 2012). The method presented in this study takes advantage of the PCF routine to evaluate bacterial distributions on surfaces over time and to identify the point of transition from random to non-random processes.

Null-model

In order to determine statistically significant differences between a completely random distribution and the experimentally observed distributions of bacteria, an adequate null hypothesis has to be established. In the present case, a hard-core effect has been observed due to the reduction of the finite geometries of bacteria to distinct centers. Allowing distances between points in the null-model of less than the least possible distance between bacterial cells (due to their physical appearance) would lead to a falsely decreased point density in the outer rings.

Therefore, a hard-core null-model with an exclusion length of 0.8 µm is used, owing to the minor axis length of the rod-shaped *E. coli*, which is between 0.6 and 1.2 µm (Mitik-Dineva et al. 2009; Hsu et al. 2013). The exclusion length represents the closest possible distance between two *E. coli* cells, lying adjacent to each other with their major axes in parallel. The PCFs of the images show no significant difference within the first 0.8 µm, emphasizing the suitability of the selected hard-core distance (see Figure 3). The exclusion length is straightforwardly incorporated to generate the confidence envelopes.

Following Wiegand et al. (2006), 99 point patterns were generated using the null hypothesis and the PCF was calculated. The 95% confidence interval was determined by taking the fifth lowest and fifth highest value for each $g(r)$ (Wiegand & Moloney 2004; Wiegand et al. 2006).

The maximum distance of the PCFs is limited to 10 µm (see Figure 3). Larger bacterial densities (micro-colonies > 10 µm) are not treatable with the method used due to possible fusion of the micro-colonies. The transition between the prevalence of random and non-random processes occurs at times where the cluster distances were in the range 0.8–10 µm.

The validity and capabilities of the presented point pattern analysis algorithm for the given bacterial densities are discussed on the basis of artificial point patterns that were generated and processed *via* the analysis pipeline. For details see Supplementary information.

Summary of the replicates

The data handling of the analysis from replicated point patterns is often complex (Diggle et al. 2000; Bell & Grunwald 2004). For the pooling of the data from different replicates, a histogram summary has been applied (see Figure 3). The $g(r)$ values for every point pattern (image) that are significantly different from that of the null-model are counted and summarized as fractions (of the pool of replicates) within this histogram. A value of 0.5 corresponds to 50% of point patterns (images) that are significantly different from the null hypotheses in the respective ring. Therefore, the bins of the histogram represent the rings for which the PCF is calculated (see Equation 1 and Figure 2). The width of the rings equals dr (0.35 µm) and the maximum distance r_{max} is 10 µm. An example of a sequence of the point pattern analysis is shown in Figure 3.

Results

For early stages of surface colonization, the allocation of bacterial cells on TiO_2 cannot be distinguished from an entirely random distribution (Figure 3). After ~9 h, the PCF method detects more neighboring bacterial cells within short distances (1–4 µm) from bacterial cells than predicted by an entirely random distribution (Figure 3, gray envelopes). This indicates a shift to a non-random pattern, where cells begin to arrange themselves in clusters. Evaluation of CLSM images derived from later colonization reveal that also at medium and relatively long distances (1–10 µm) the number of bacterial cells is higher than expected in a random distribution. The fraction of annuli was calculated deviating from the random distribution to illustrate the progressive growth of bacterial clusters (Figure 3, Summary). This procedure was done for all four materials and each time point, and was summarized as an increasing 'degree of non-randomness' during the progress of surface colonization (Figure 4, right panels).

Comparison of bacterial colonization kinetics (derived from the CLSM images) and the PCF summary reveals two prevailing processes (observable by different slopes): a non-dominant random adhesion behavior and a dominant non-random behavior. The dominant non-random behavior may result from bacterial growth on the surface, cooperative adhesion or a combination of both (Figure 4).

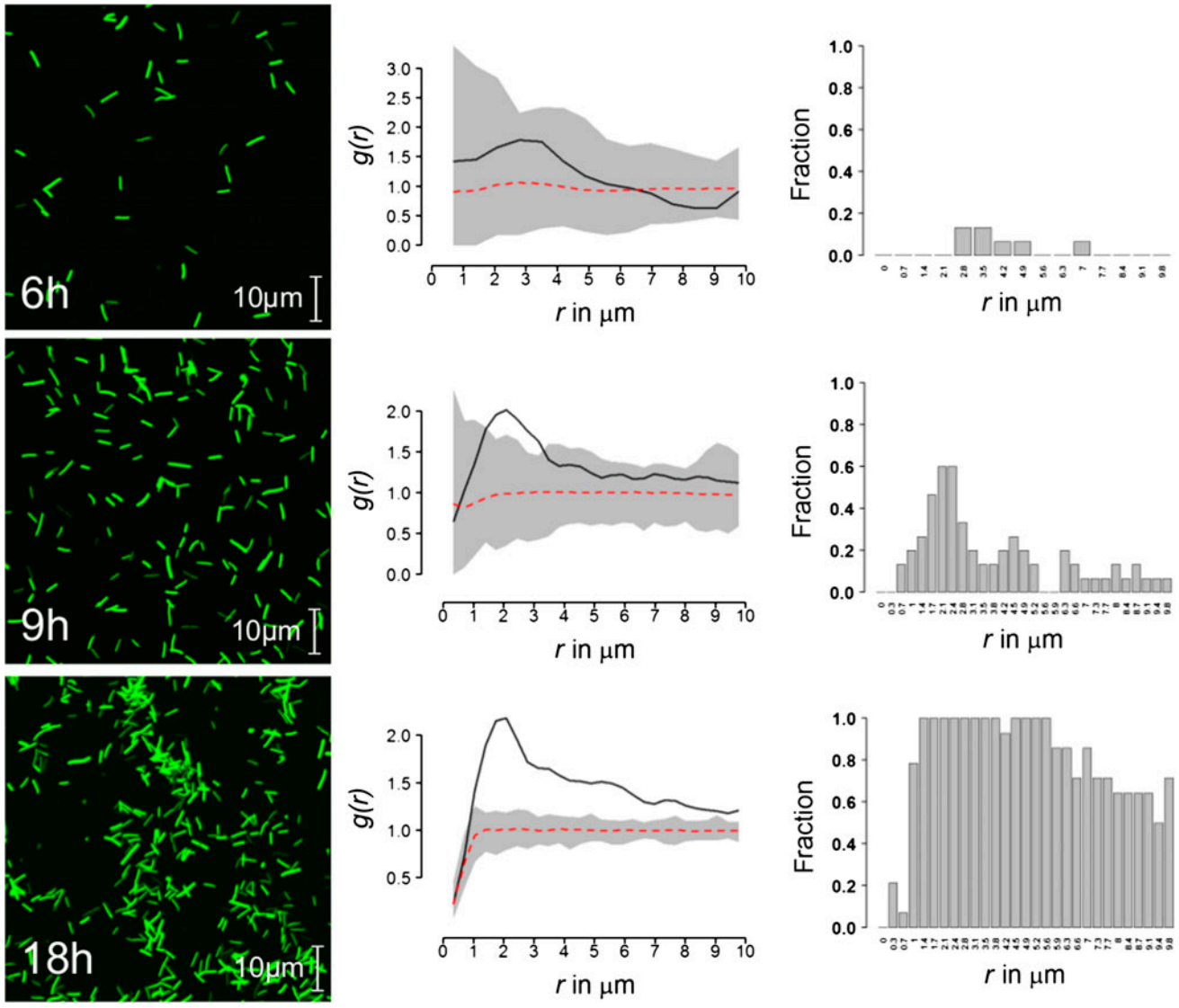

Figure 3. Point pattern analysis at three different points in time of adhesion of *E. coli* on a TiO_2 surface. Left column: exemplative CLSM image for the respective point in time. Middle column: the corresponding PCFs (black curve: PCF of the left CLSM image; gray curves: significance envelope of the null-model). If PCF is outside the envelope, the distribution of bacterial cells is significantly different from a randomly distributed pattern ($p < 0.05$). Right column: summary of the PCFs of all CLSM images showing the fraction of investigated annuli, deviating from a random distribution.

Furthermore, the inherent differences in the respective adhesion processes on the four substrata are obvious. Random adhesion behavior of *E. coli* cells is observable up to different time points on the tested surfaces ranging from 2 h (PTFE) to 30 h (glass). The change to the predominance of non-random processes (eg cooperative adhesion or growth) within the observation period exhibits approximately the same value for TCPS and Ti (≈ 6–9 h), whereas the transition is faster for PTFE (2–3 h) and much slower for the glass surface (30–38 h) (see Figure 4).

A positive correlation was observed between cluster size (derived from image processing) and the degree of non-randomness of bacterial distribution for all four materials (see Figure 5). The cluster sizes for all points in time range from ~2–6 bacteria per cluster for glass, TCPS and TiO_2 to ~2–17 bacteria per cluster for PTFE. Accordingly, PTFE exhibits the highest density of bacterial clusters (2.09 bacteria μm^{-2}) compared to glass, TCPS of TiO_2 with bacterial densities ranging from 0.74 to 1.07 bacteria μm^{-2} (see Table 1).

In order to analyze the effect of surface properties on the bacterial size (see Figure 6), bacterial cell sizes were derived from the respective covered surface area which is accessible *via* image processing (details of the exact image processing method for the determination of the additional parameters shown in Figures 5, 6 and Table 1

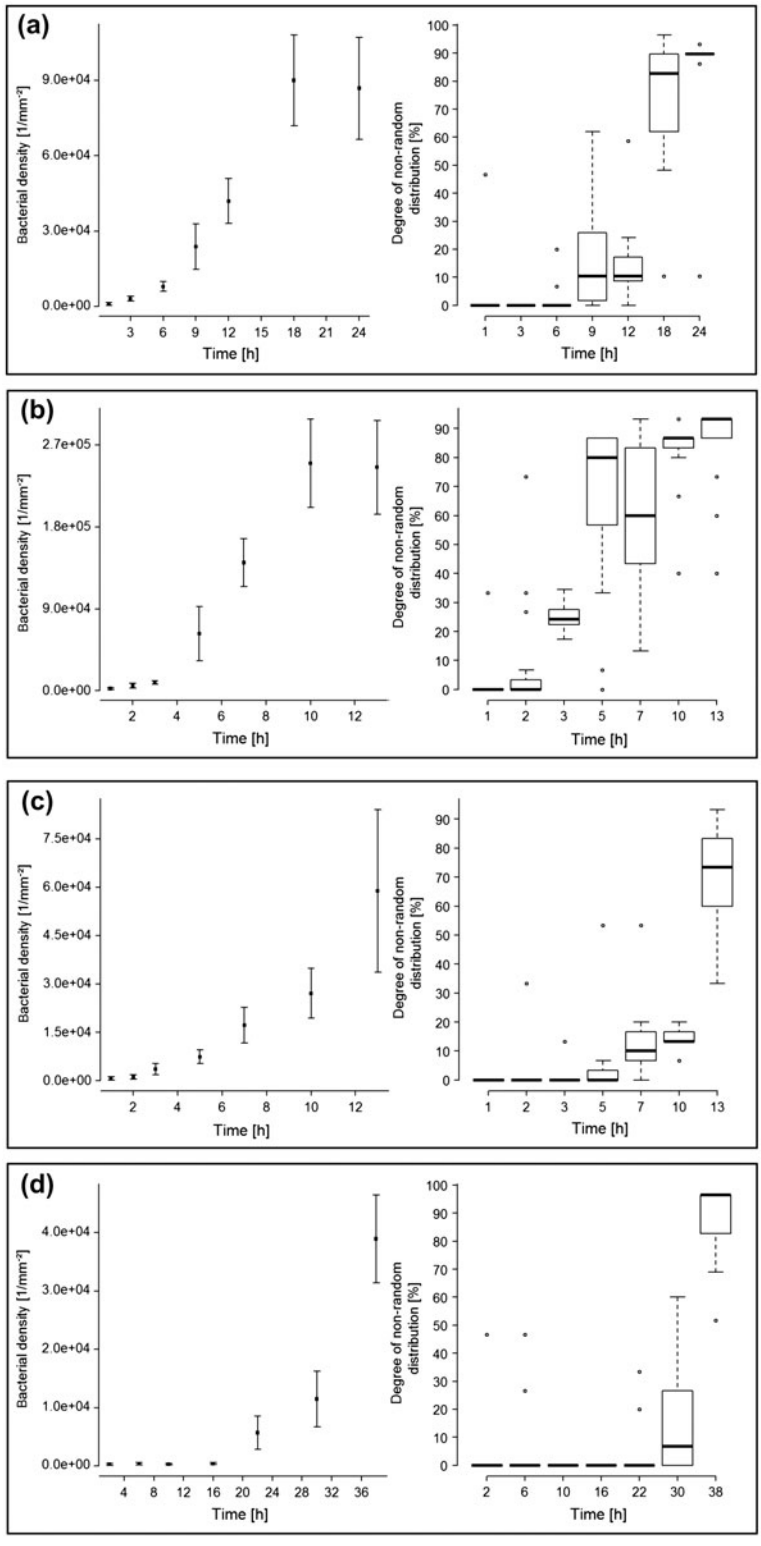

Figure 4. Adhesion kinetics derived from image analysis (left panel) and corresponding summary of PCF statistics (right panel) for four different materials. (a) TiO_2; (b) PTFE; (c) TCPS; (d) glass. Boxplots show the degree of non-random distribution of bacterial cells derived from the summary histogram (an example is shown for TiO_2 in Figure 3). Note the similar trends in the kinetics and statistical analysis (see text for further details).

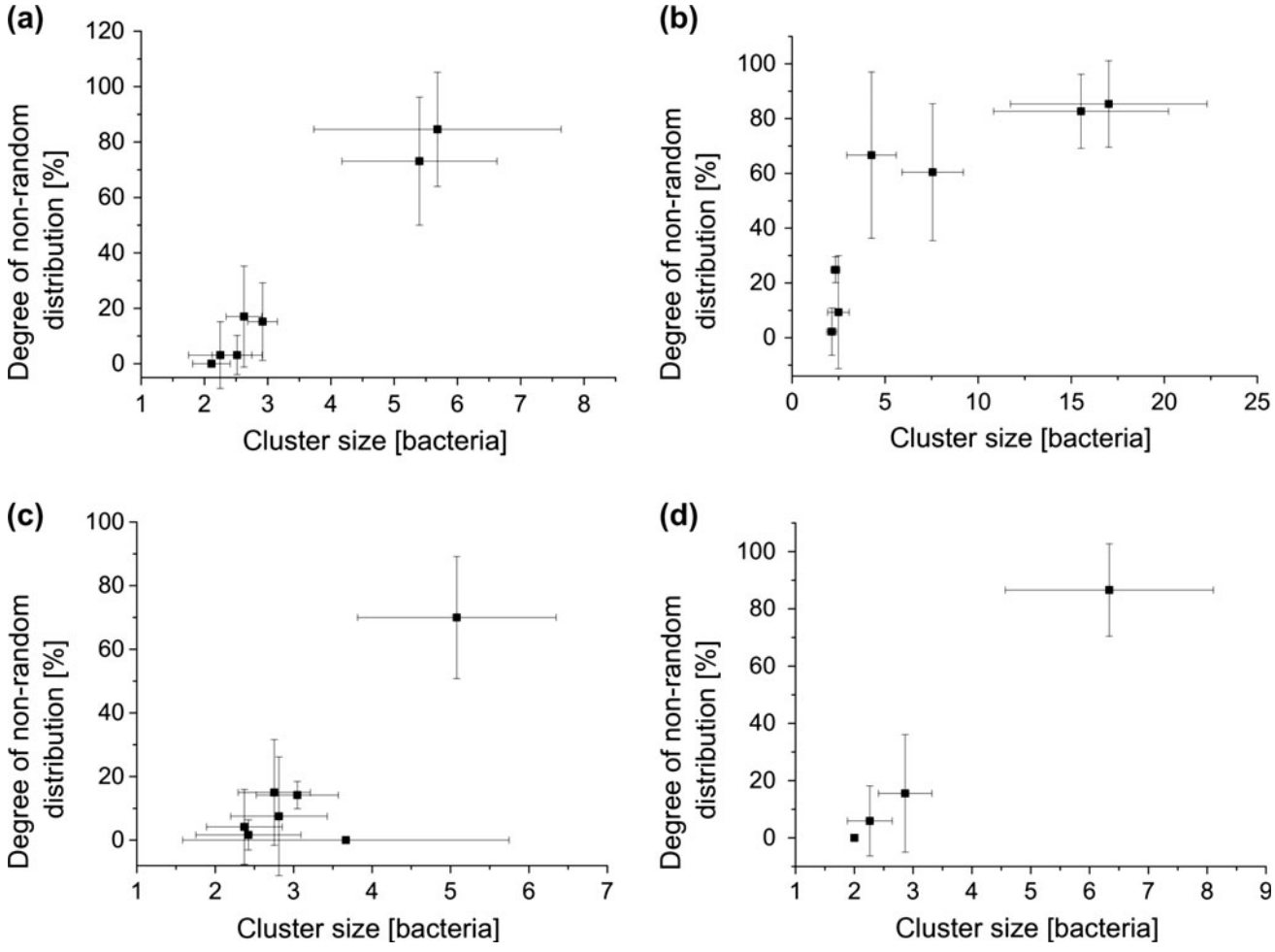

Figure 5. Correlation between the mean size of bacterial clusters and the degree of non-randomness determined *via* PCF statistics for four different surfaces. (a) TiO_2; (b) PTFE; (c) TCPS; (d) glass. Error bars correspond to SD. For details of the image processing to determine the cluster size see Supplementary information.

Table 1. Mean cluster density for the bacteria adhered to the four materials determined *via* image processing.*

	Mean cluster density (bacteria μm^{-2})
TiO_2	1.07
TCPS	0.95
PTFE	2.09
Glass	0.74

*For details see Supplementary information: mean values of all points in time and all images.

can be found in the Supplementary information). Cell sizes are displayed for two different points in time: $t_{initial}$ represents the bacterial sizes of the two first points in time per material (TiO_2, PTFE, TCPS: 1 and 2 h; glass: 2 and 6 h) and t_{final} represents the bacterial sizes of the single cells for the last point in time for the respective material (TiO_2: 18 h; PTFE, TCPS: 13 h; glass: 38 h). Cell sizes for $t_{initial}$ are not significantly different (Kruskal–Wallis test, $p = 0.41$), whereas significant deviations for t_{final} are detected (Kruskal–Wallis test, $p < 2.2 \times 10^{-16}$). Finally, a significant decrease was detected in cell size during colonization for all investigated materials, except for glass (Mann–Whitney U test, TiO_2: $p < 2.0 \times 10^{-6}$, PTFE: $p < 6.4 \times 10^{-16}$, TCPS: $p < 2.0 \times 10^{-6}$, glass: $p = 0.9$).

The application of CLSM is susceptible to measurement errors in the case of large micro-colonies that exhibit three-dimensional expansion. This is due to the fact that CLSM images represent a near-surface slice of the bacterial micro-colony und thus potentially underestimate the total bacterial colonization. This leads to a measured constant number of attached bacteria in the last points in time (24 and 13 h, respectively; see Figure 4) for TiO_2 and PTFE. The method presented in this study is in general tailored for the early stages of biofilm development, ie from bacterial adhesion to the formation of micro-colonies, where the transition between prevailing random and non-random processes occurs.

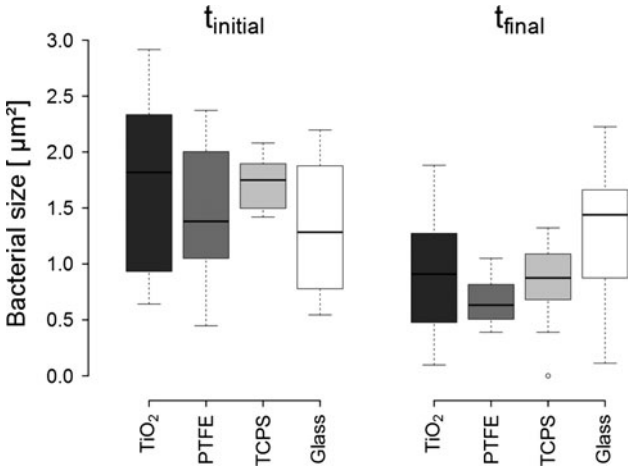

Figure 6. Boxplots of the different cell sizes of single bacterial cells for the early ($t_{initial}$) and late (t_{final}) points in time for the different materials. At $t_{initial}$ all single bacterial cells within the images for the first two points in time for the respective material (TiO_2, PTFE, TCPS: 1 and 2 h; glass: 2 and 6 h) are evaluated. In contrast, t_{final} encompasses all single bacterial cells within the images for the last point in time for the respective material (TiO_2: 18 h; PTFE, TCPS: 13 h; glass: 38 h). At t_{final} the mean bacterial size differs significantly between the observed materials (Kruskal–Wallis, $p < 2.2 \times 10^{-16}$) but not at $t_{initial}$ (Kruskal–Wallis, $p = 0.41$). All materials, except glass, show a significant decrease in the bacterial size (see text for further details). The cell sizes shown here correspond to the respective projected cell areas accessible *via* image processing.

Discussion

The present study aims at discriminating between prevalently random and non-random processes (eg cooperative adhesion and growth) at early stages of surface colonization by applying a novel point pattern analysis algorithm to rod-shaped bacteria adhered to the biomaterial surfaces. Thus an objective criterion was provided to detect cluster formation. A model system of *E. coli* and four different biomaterials was used. The novelty is the image processing routine with subsequent statistical analysis of spatial point patterns. Distinguishing possible reasons for random or non-random behavior during early bacterial colonization was not the focus of the study, and detailed conclusions about this cannot yet be drawn. In general, two processes are most likely to cause non-random behavior: growth of bacteria at the material surface, and preferential adhesion of planktonic bacteria to already attached bacteria. The latter may be induced by quorum sensing, for example.

Significance of the point pattern analysis for application to early bacterial colonization

At the early stages of colonization, the calculations for the TiO_2 surface (see Figure 3) show no or only a few rings with small r values that do not fall into the range of variations of the random null-model. This is in agreement with results in the literature that identified initial adhesion processes of bacteria to solid surfaces to be random in colloid systems (Beloin et al. 2008). Later stages of colonization show an increasing fraction of rings that cannot be described by the random null-model, indicating non-random processes.

Dependency of the transition behavior with respect to material properties

With the method presented here it is possible to access quantitatively the transition from random to non-random processes on different classes of biomaterials. Gottenbos et al. (2000) described the dependency of the transition for one class of biomaterials (polymeric), considering the change between bacterial adhesion (random) and growth (non-random) by applying real-time image analysis to parallel plate flow chamber experiments. Gottenbos et al. (2000) showed that the growth parameters for *Staphylococcus epidermidis*, eg generation time, depend on the chemistry of the polymeric surface. Thus, the hydrophobicity of the surface influences the growth of micro-colonies: increasing the hydrophobicity of a surface accelerates bacterial growth (Gottenbos et al. 2000). In the present study it was also found that hydrophobic surfaces accelerated the transition from random to non-random behavior. The water contact angles of the material surfaces, which are a measure of hydrophobicity, were: $113.2° \pm 0.8°$ (PTFE); $88.0° \pm 1.8$ (TCPS); $74.3° \pm 4.9°$ (TiO_2); $32.7° \pm 2°$ (glass) [for further details of the surface characterization see Lüdecke et al. (2014)]. As mentioned above, the transition between random and non-random processes occurs earlier for more hydrophobic surfaces: after 2–3 h for PTFE; 5–7 h for TCPS; 6–9 h for TiO_2 and 30–38 h for glass (see Figure 4). This is in good agreement with other experimental studies showing a similar qualitative trend (Tegoulia & Cooper 2002; Parreira et al. 2011).

As mentioned earlier, a detailed analysis of the underlying mechanisms responsible for the shift from random to non-random behavior is not the aim of the study, but possible general aspects are discussed briefly, as follows. Differences in the hydrophobicity of the surfaces are an explanation for the different transition point in time between random and non-random behavior. As shown by different studies, the binding forces of bacteria to hydrophobic surfaces are usually stronger than to hydrophilic surfaces (Boks, Busscher et al. 2008, 2009). Consequentially, the attachment of bacteria to hydrophobic surfaces tends to be irreversible and the bacteria are immobile, showing less bond-maturation (Boks, Norde et al. 2008, 2009). Following Busscher and Van der Mei (2012), hydrophobic surfaces can provide a better ‘force

environment' for biofilm development. Both the faster immobile adhesion and the better force environment would lead to a faster metabolic switch of adhered bacteria on hydrophobic surfaces and consequently a faster transition between a random and non-random regime. In this study the adhesion behavior of the materials is different, with the fastest adhesion on PTFE (see left column in Figure 4). The degree of non-random adhesion with respect to bacterial density does not suggest the existence of a distinct transition point at one particular bacterial density. For all materials, the transition occurs at different bacterial densities. Thus, the range of bacterial density (1×10^4 bacteria mm^{-2} to 4.5×10^4 bacteria mm^{-2}) indicates that the transition between random and non-random processes is not governed by the number of adhered bacteria.

Biological implications of parameters derived from point pattern analysis and image processing

Recent studies of biofilm formation on engineered surfaces suggest that the spatial distribution and the size of micro-colonies are crucial for the development of mature biofilms (Gu et al. 2013; Perni & Prokopovich 2013). Shorter distances between the micro-colonies are expected to accelerate biofilm formation (Gu et al. 2013). The present results support these findings: surfaces with a high number of attached bacteria and a high number of clusters (eg PTFE) show a faster transition from random to non-random processes, which would also result in accelerated biofilm formation (see Figures 4 and 5). Additionally, the dynamics of the increase in the cluster size is in good agreement with data derived from the PCF. In addition to second order statistics, image processing was applied to obtain information regarding the morphology of the bacterial cells and clusters (see Table 1 and Figure 6). Interestingly, the mean cell size of bacteria differs on the investigated surfaces, especially for the late time points (see Figure 6).

The design of the present experiment (continuous bacterial culture) allows the generation of planktonic cells in a similar physiological state, ie with similar morphology, as a starting point for the adhesion experiments (Lüdecke et al. 2014). This is consistent with the image analysis showing that the size of attached single cells is not statistically different at early points in time (see Figure 6). Accordingly, the substratum chemistry and topography are the driving forces for the change in cell morphology. In the present study, the cell size at the latest point in time on the polymeric substrate (TCPS: 0.86 μm^2; PTFE: 0.64 μm^2) is smaller than on all other substrata (TiO_2: 0.93 μm^2; glass: 1.21 μm^2). Differences in cell size have been observed for different substrata (Mitik-Dineva et al. 2009; Hsu et al. 2013). The distinct differences in cell morphology may arise as a response to different stress states on the different substratum materials, triggered eg by differences in nutrient availability at the surface, or by differences in the forces acting on the bacterial cells (see section above) (Young 2006). For *Helicobacter pylori*, the cell shape is significantly different when cells adhered to metallic or polymeric surfaces, and also differs between a spiral shape on hydrophobic self-assembled monolayers (SAMs) and a coccoid shape on hydrophilic SAMs (Azevedo et al. 2007; Parreira et al. 2011). In addition, image analysis of attached *Acinetobacter* sp. on glass surfaces shows a dependency of cell size on nutrient availability, with smaller cell sizes during starvation (James et al. 1995). A general correlation regarding the type of surfaces on which the respective cells are more viable has to be the topic of further studies. The correlation between bacterial cell sizes at t_{final} and the hydrophobicity of the material is obvious: the more hydrophilic the material the larger the cell size of single bacterial cells. This emphasizes the effect of the different forces (which are higher on hydrophobic surfaces) on the cell response and cluster density (see Table 1 and Figure 6). This bacterial density is also distinctly correlated with resistance to antibiotic treatment and immune defense (Gristina 1987; Stewart & Costerton 2001; Davies 2003). Furthermore, the difference in morphology of bacterial cells and micro-colonies (size, density) indicates that the success of antibiotic treatment is likely to be dependent on the material where the biofilm is established.

As discussed by Van der Mei and Busscher (2012), bacterial cell heterogeneity is a possible cause for different cell morphologies being present on different biomaterials. Especially on PTFE, low cell size was found to be accompanied by a large number of bacteria per cluster, leading to high cluster densities (see Figure 5 and Table 1).

The results clearly show that not only are bacterial adhesion and the subsequent build-up of micro-colonies influenced by the respective substratum, but also the transition points in time between both these processes. Accordingly, the novel point pattern analysis method introduced in this study indicates a suitable time frame for the application of antibiotic agents for the treatment of biofilms.

Summary

With the application of point pattern analysis and PCFs, random adhesion and non-random processes (cooperative adhesion or growth) during the early stages of bacterial biofilm formation are separated. Random adhesion is followed by non-random processes for all investigated materials. The authors were able to characterize the transition between both processes quantitatively which had, to their best knowledge, not been accomplished in

previous studies. Thus, an objective criterion for distinguishing random from non-random processes is provided. Furthermore, image processing revealed differences in cell and cluster morphologies on the different biomaterials. Together with the differences in the change of the surface colonization mechanism, this has important consequences for successful treatment of biomaterial-associated infections of implants by antibiotics.

Acknowledgements

This work was supported by the Jena School for Microbial Communication (JSMC/MikroInter) funded by the DFG and the State of Thuringia. Fruitful discussions with J. Schleicher and M. Föge are gratefully acknowledged.

References

Azevedo NF, Almeida C, Cerqueira L, Dias S, Keevil CW, Vieira MJ. 2007. Coccoid form of *Helicobacter pylori* as a morphological manifestation of cell adaptation to the environment. Appl Environ Microbiol. 73:3423–3427.

Baddeley A, Turner R. 2005. spatstat: an R package for analyzing spatial point patterns. J Stat Softw. 12:1–42.

Barton AJ, Sagers RD, Pitt WG. 1996. Measurement of bacterial growth rates on polymers. J Biomed Mater Res. 32:271–278.

Bell ML, Grunwald GK. 2004. Mixed models for the analysis of replicated spatial point patterns. Biostatistics. 5:633–648.

Beloin C, Houry A, Froment M, Ghigo J-M, Henry N. 2008. A short-time scale colloidal system reveals early bacterial adhesion dynamics. PLoS Biol. 6:e167.

Boks NP, Busscher HJ, Van der Mei HC, Norde W. 2008. Bond-strengthening in staphylococcal adhesion to hydrophilic and hydrophobic surfaces using atomic force microscopy. Langmuir. 24:12990–12994.

Boks NP, Kaper HJ, Norde W, Van der Mei HC, Busscher HJ. 2009. Mobile and immobile adhesion of staphylococcal strains to hydrophilic and hydrophobic surfaces. J Colloid Interf Sci. 331:60–64.

Boks NP, Norde W, Van der Mei HC, Busscher HJ. 2008. Forces involved in bacterial adhesion to hydrophilic and hydrophobic surfaces. Microbiol-Sgm. 154:3122–3133.

Bos R, Van der Mei HC, Meinders JM, Busscher HJ. 1994. A quantitative method to study co-adhesion of microorganisms in a parallel plate flow chamber: basic principles of the analysis. J Microbiol Methods. 20:289–305.

Busscher HJ, Van der Mei HC. 2012. How do bacteria know they are on a surface and regulate their response to an adhering state? Plos Pathogens. Jan;8.

Busscher HJ, Van der Mei HC, Subbiahdoss G, Jutte PC, van den Dungen JJAM, Zaat SAJ, Schultz MJ, Grainger DW. 2012. Biomaterial-associated infection: locating the finish line in the race for the surface. Sci Transl Med. 4:p153rv10.

Costerton JW, Stewart PS, Greenberg EP. 1999. Bacterial biofilms: acommon cause of persistent infections. Science. 284:1318–1322.

Davies D. 2003. Understanding biofilm resistance to antibacterial agents. Nat Rev Drug Discov. 2:114–122.

Diggle PJ, Mateu J, Clough HE. 2000. A comparison between parametric and non-parametric approaches to the analysis of replicated spatial point patterns. Advs Appl Probab. 32:331–343.

Gibiansky ML, Conrad JC, Jin F, Gordon VD, Motto DA, Mathewson MA, Stopka WG, Zelasko DC, Shrout JD, Wong GCL. 2010. Bacteria use Type IV pili to walk upright and detach from surfaces. Science. 330:197–U150.

Giraldez MJ, Resua CG, Lira M, Oliveira MECDR, Magariños B, Toranzo AE, Yebra-Pimentel E. 2010. Contact lens hydrophobicity and roughness effects on bacterial adhesion. Optom Vis Sci. 87:E426–E431.

Gottenbos B, Busscher HJ, Van der Mei HC. 2002. Pathogenesis and prevention of biomaterial centered infections. J Mater Sci – Mater Med. 13:717–722.

Gottenbos B, Van der Mei HC, Busscher HJ. 2000. Initial adhesion and surface growth of *Staphylococcus epidermidis* and *Pseudomonas aeruginosa* on biomedical polymers. J Biomed Mater Res. 50:208–214.

Gristina AG. 1987. Biomaterial-centered infection: microbial adhesion versus tissue integration. Science. 237:1588–1595.

Grivet M, Morrier J-J, Souchier C, Barsotti O. 1999. Automatic enumeration of adherent streptococci or actinomyces on dental alloy by fluorescence image analysis. J Microbiol Methods. 38:33–42.

Gu H, Hou S, Yongyat C, De Tore S, Ren D. 2013. Patterned biofilm formation reveals a mechanism for structural heterogeneity in bacterial biofilms. Langmuir. 29:11145–11153.

Gustafson DE, Kessel WC. 1979. Fuzzy clustering with a fuzzy covariance matrix. In: Proceedings of the IEEE Conference on Decision and Control, San Diego, CA; p. 761–766.

Hamilton MA, Johnson KR, Camper AK, Stoodley P, Harkin GJ, Gillis RJ, Shope PA. 1995. Analysis of bacterial spatial patterns at the initial stage of biofilm formation. Biom J. 37:393–408.

Hsu LC, Fang J, Borca-Tasciuc DA, Worobo RW, Moraru CI. 2013. Effect of micro- and nanoscale topography on the adhesion of bacterial cells to solid surfaces. Appl Environ Microbiol. 79:2703–2712.

Ivanova EP, Truong VK, Wang JY, Berndt CC, Jones RT, Yusuf II, Peake I, Schmidt HW, Fluke C, Barnes D, et al. 2010. Impact of nanoscale roughness of titanium thin film surfaces on bacterial retention. Langmuir. 26:1973–1982.

James GA, Korber DR, Caldwell DE, Costerton JW. 1995. Digital image-analysis of growth and starvation responses of a surface-colonizing *Acinetobacter* sp. J Bacteriol. 177:907–915.

Katsikogianni M, Missirlis YF. 2004. Concise review of mechanisms of bacterial adhesion to biomaterials and of techniques used in estimating bacteria-material interactions. Eur Cell Mater. 8:37–57.

Law R, Illian J, Burslem DFRP, Gratzer G, Gunatilleke CVS, Gunatilleke IAUN. 2009. Ecological information from spatial patterns of plants: insights from point process theory. J Ecol. 97:616–628.

Lüdecke C, Bossert J, Roth M, Jandt KD. 2013. Physical vapor deposited titanium thin films for biomedical applications: reproducibility of nanoscale surface roughness and microbial adhesion properties. Appl Surf Sci. 280:578–589.

Lüdecke C, Jandt KD, Siegismund D, Kujau MJ, Zang E, Rettenmayr M, Bossert J, Roth M. 2014. Reproducible biofilm cultivation of chemostat-grown *Escherichia coli* and investigation of bacterial adhesion on biomaterials using a non-constant-depth film fermenter. PLoS ONE. 9:e84837.

McQuarrie DA. 1975. Statistical mechanics. New York: Harper & Row.

Medilanski E, Kaufmann K, Wick LY, Wanner O, Harms H. 2002. Influence of the surface topography of stainless steel on bacterial adhesion. Biofouling. 18:193–203.

Mitik-Dineva N, Wang J, Truong VK, Stoddart P, Malherbe F, Crawford RJ, Ivanova EP. 2009. *Escherichia coli, Pseudomonas aeruginosa*, and *Staphylococcus aureus* attachment patterns on glass surfaces with nanoscale roughness. Curr Microbiol. 58:268–273.

Otsu N. 1979. A threshold selection method from gray-level histograms. IEEE Trans Syst, Man, Cybern. 9:62–66.

Parreira P, Magalhaes A, Goncalves IC, Gomes J, Vidal R, Reis CA, Leckband DE, Martins MCL. 2011. Effect of surface chemistry on bacterial adhesion, viability, and morphology. J Biomed Mater Res Part A. 99A:344–353.

Parreira P, Magalhães A, Gonçalves IC, Gomes J, Vidal R, Reis CA, Leckband DE, Martins MCL. 2011. Effect of surface chemistry on bacterial adhesion, viability, and morphology. J Biomed Mater Res A. 99:344–353.

Perni S, Prokopovich P. 2013. Micropatterning with conical features can control bacterial adhesion on silicone. Soft Matter. 9:1844–1851.

Ploux L, Beckendorff S, Nardin M, Neunlist S. 2007. Quantitative and morphological analysis of biofilm formation on self-assembled monolayers. Colloids Surf B Biointerfaces. 57:174–181.

Ponche A, Bigerelle M, Anselme K. 2010. Relative influence of surface topography and surface chemistry on cell response to bone implant materials. Proc Inst Mech Eng H. 224:1471–1486.

Renner LD, Weibel DB. 2011. Physicochemical regulation of biofilm formation. MRS Bull. 36:347–355.

Ripley BD. 1977. Modeling spatial patterns. J Roy Stat Soc B Met. 39:172–212.

Schillinger C, Petrich A, Lux R, Riep B, Kikhney J, Friedmann A, Wolinsky LE, Gäbel UB, Daims H, Moter A. 2012. Co-localized or randomly distributed? Pair cross correlation of in vivo grown subgingival biofilm bacteria quantified by digital image analysis. PLoS ONE. 7:e37583.

Schleicher J, Wiegand K, Ward D. 2011. Changes of woody plant interaction and spatial distribution between rocky and sandy soil areas in a semi-arid savanna, South Africa. J Arid Environ. 75:270–278.

Siegismund D, Undisz A, Germerodt S, Schuster S, Rettenmayr M. 2014. Quantification of the interaction between biomaterial surfaces and bacteria by 3-D modeling. Acta Biomater. 10:267–275.

Singh AV, Vyas V, Patil R, Sharma V, Scopelliti PE, Bongiorno G, Podestà A, Lenardi C, Gade WN, Milani P. 2011. Quantitative characterization of the influence of the nanoscale morphology of nanostructured surfaces on bacterial adhesion and biofilm formation. PLoS ONE. 6:e25029.

Sjollema J, Busscher HJ. 1990. Deposition of polystyrene particles in a parallel plate flow cell. 2. Pair distribution-functions between deposited particles. Coll and Surf. 47:337–352.

Sjollema J, Van der Mei HC, Uyen HM, Busscher HJ. 1990. Direct observations of cooperative effects in oral streptococcal adhesion to glass by analysis of the spatial arrangement of adhering bacteria. FEMS Microbiol Lett. 69:263–269.

Stewart PS, Costerton WJ. 2001. Antibiotic resistance of bacteria in biofilms. Lancet. 358:135–138.

Taylor JR. 1997. An introduction to error analysis : the study of uncertainties in physical measurements. 2nd ed. Sausalito (CA): University Science Books.

Tegoulia VA, Cooper SL. 2002. *Staphylococcus aureus* adhesion to self-assembled monolayers: effect of surface chemistry and fibrinogen presence. Colloids Surf B. 24:217–228.

Van der Mei HC, Busscher HJ. 2012. Bacterial cell surface heterogeneity: a pathogen's disguise. PLoS Pathog. 8: e1002821.

Van der Mei HC, Cox SD, Geertsema-Doornbusch GI, Doyle RJ, Busscher HJ. 1993. A critical-appraisal of positive cooperativity in oral streptococcal adhesion – scatchard analyses of adhesion data versus analyses of the spatial arrangement of adhering bacteria. J Gen Microbiol. 139:937–948.

Wiegand T, Moloney KA. 2004. Rings, circles, and null-models for point pattern analysis in ecology. Oikos. 104:209–229.

Wiegand T, Kissling WD, Cipriotti PA, Aguiar MR. 2006. Extending point pattern analysis for objects of finite size and irregular shape. J Ecol. 94:825–837.

Young KD. 2006. The selective value of bacterial shape. Microbiol Mol Biol R. 70:660.

Zhao K, Tseng BS, Beckerman B, Jin F, Gibiansky ML, Harrison JJ, Luijten E, Parsek MR, Wong GCL. 2013. Psl trails guide exploration and microcolony formation in *Pseudomonas aeruginosa* biofilms. Nature. 497:388–391.